NANO IDEAS

Influence of Uniaxial Tensile Stress on the Mechanical and Piezoelectric Properties of Short-period Ferroelectric Superlattice

Yifeng Duan · Chunmei Wang · Gang Tang · Changqing Chen

Abstract Tetragonal ferroelectric/ferroelectric $BaTiO_3$/$PbTiO_3$ superlattice under uniaxial tensile stress along the c axis is investigated from first principles. We show that the calculated ideal tensile strength is 6.85 GPa and that the superlattice under the loading of uniaxial tensile stress becomes soft along the nonpolar axes. We also find that the appropriately applied uniaxial tensile stress can significantly enhance the piezoelectricity for the superlattice, with piezoelectric coefficient d_{33} increasing from the ground state value by a factor of about 8, reaching 678.42 pC/N. The underlying mechanism for the enhancement of piezoelectricity is discussed.

Keywords Mechanical property · Piezoelectricity · Ferroelectric superlattice

Introduction

Ferroelectrics, which can convert mechanical to electrical energy (and vice versa) have wide applications in medical imaging, telecommunication and ultrasonic devices, the physical properties of which are sensitive to external conditions, such as strain, film thickness, temperature, electric and magnetic fields [1–3]. $BaTiO_3$ (BTO) and $PbTiO_3$ (PTO), as prototype ferroelectric materials and simple systems, have been intensively studied [4, 5]. It is known that the ferroelectricity arises from the competition of short-range repulsions which favor the paraelectric cubic phase and Coulomb forces, which favor the ferroelectric phase [6, 7]. As the pressure increases, the short-range repulsions increase faster than the Coulomb forces, leading to the reduced ferroelectricity. Accompanied with the suppression of ferroelectricity, the piezoelectricity decreases and even disappears. However, recent studies have shown that the noncollinear polarization rotation, occurring at phase transition pressure, can result in the giant piezoelectric response [8, 9]. In contrast to previous theoretical studies of the effects of epitaxial strain on the spontaneous polarization of ferroelectric thin films, we have systematically studied the influence of uniaxial and in-plane epitaxial strains on the mechanical and piezoelectric properties of perovskite ferroelectrics [10–15]. So far, there has been no previous work on the effect of uniaxial tensile strains on the mechanical and piezoelectric properties of short-period BTO/PTO superlattices.

Ferroelectric superlattices composed of alternating epitaxial oxides ultrathin layers are currently under intensive study due to their excellent ferroelectric and piezoelectric properties [16]. Ferroelectricity can be induced in AB_1O_3/AB_2O_3 superlattice in spite of the paraelectric nature of AB_1O_3 and AB_2O_3. This is because the coincidence of the positive and negative charge centers is destroyed in the superlattice and electric dipoles are induced. Moreover, ferroelectricity can be enhanced in ferroelectric superlattices in certain stacking sequences [17]. The overall polarization of three-component $SrTiO_3$(STO)/BTO/PTO ferroelectric superlattices can also

Y. Duan (✉) · G. Tang
Department of Physics, China University of Mining and Technology, 221116 Xuzhou, People's Republic of China
e-mail: yifeng@semi.ac.cn

C. Wang
School of Aerospace, Xi'an Jiaotong University, 710049 Xi'an, People's Republic of China

C. Chen
Department of Engineering Mechanics, AML, Tsinghua University, 100084 Beijing, People's Republic of China
e-mail: chencq@tsinghua.edu.cn

be improved by increasing the number of BTO and PTO layers [18]. Thanks to the periodic nature, it is possible to study the effect of uniaxial or biaxial strains on the properties of ferroelectric superlattices from first principles.

In this work, we perform total energy as well as linear response calculations to study the effect of uniaxial tensile stress along the c axis on the mechanical and piezoelectric properties of short-period BTO/PTO superlattice. We show the mechanical properties by calculating the ideal tensile strength, elastic constants and valence charge density at different strains. We also show the influence of uniaxial stress on the piezoelectricity. To reveal the underlying mechanisms, we study the effects of uniaxial tensile stress on the atomic displacements and Born effective charges, respectively.

Computational Methods

Our calculations are performed within the local density approximation (LDA) to the density functional theory (DFT) as implemented in the plane-wave pseudopotential ABINIT package [19]. To ensure good numerical convergence, the plane-wave energy cutoff is set to be 80 Ry, and the Brillouin zone integration is performed with $6 \times 6 \times 6$ **k**-meshpoints. The norm-conserving pseudopotentials generated by the OPIUM program are tested against the all-electron full-potential linearized augmented plane-wave method [20, 21]. The orbitals of Ba $5s^2 5p^6 6s^2$, Pb $5d^{10} 6s^2 6p^2$, Ti $3s^2 3p^6 3d^2 4s^2$ and O $2s^2 2p^4$ are explicitly included as valence electrons. The dynamical matrices and Born effective charges are computed by the linear response theory of strain type perturbations, which has been proved to be highly reliable for ground state properties [22–24]. The polarization is calculated by the Berry-phase approach [25]. The LDA is used instead of the generalized gradient approximation (GGA) because the GGA is found to overestimate both the equilibrium volume and strain for the perovskite structures [26]. The piezoelectric strain coefficients $d_{iv} = \Sigma_{\mu=1}^6 e_{i\mu} s_{\mu v}$, where **e** is the piezoelectric stress tensor and the elastic compliance tensor **s** is the reciprocal of the elastic stiffness tensor **c** (Roman indexes from 1 to 3, and Greek ones from 1 to 6).

In the calculations, a double-perovskite ten-atom supercell along the c axis is used for the tetragonal short-period BTO/PTO superlattice. The primitive periodicity of tetragonal structure with the space group $P4mm$ is retained, which is more stable in energy than the rhombohedral structure. For the tetragonal perovskite structure compounds BTO and PTO, the equilibrium lattice parameters are $a(BTO)=3.915$ Å, $c(BTO) = 3.995$ Å, $a(PTO) = 3.843$ Å and $c(PTO) = 4.053$ Å, which are slightly less than the experimental values of 3.994, 4.034, 3.904 and
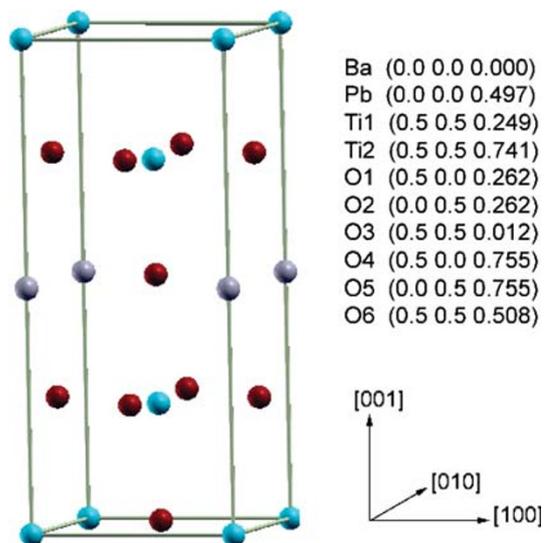

Fig. 1 The sketch of short-period ferroelectric superlattice with its atomic positions

4.135 Å, respectively [13, 14]. A sketch of ground state short-period BTO/PTO superlattice with its atomic positions is shown in Fig. 1.

To calculate the uniaxial tensile stress σ_{33}, we apply a small strain increment η_3 along the c axis and then conduct structural optimization for the lattice vectors perpendicular to the c axis, and all the internal atomic positions until the two components of stress tensor (i.e., σ_{11} and σ_{22}) are smaller than 0.05 GPa. The strain is then increased step by step. Since $\sigma_{11} = \eta_1(c_{11} + c_{12}) + \eta_3 c_{13}$, the elastic constants satisfy $\eta_3/\eta_1 \approx -(c_{11} + c_{12})/c_{13}$ under the loading of uniaxial tensile strain applied along the c axis, where the strains η_i are calculated by $\eta_1 = \eta_2 = (a - a_0)/a_0$ and $\eta_3 = (c - c_0)/c_0$, with $a_0 = 3.897$ Å and $c_0 = 7.859$ Å being the lattice constants of the unstrained superlattice structure. We have examined the accuracy of our calculations by studying the influence of different strains on the properties of BTO and PTO, respectively [12–15].

Results and Discussion

Figure 2a shows the uniaxial tensile stress σ_{33} as a function of strain η_3. The relation between strains η_1 and η_3 is shown in the inset, which satisfy $\eta_3 > -2\eta_1$. The stress σ_{33} increases until reaching its maximum value of 6.85 GPa with increasing strain, indicating that the calculated ideal tensile strength is 6.85 GPa for the superlattice, which is the maximum stress required to break the superlattice. Figure 2b shows the elastic constants as a function of stress σ_{33}, which reflect the relation between stress and strain. What is the most unexpected is that the constant c_{33} first decreases until reaching its minimum value at
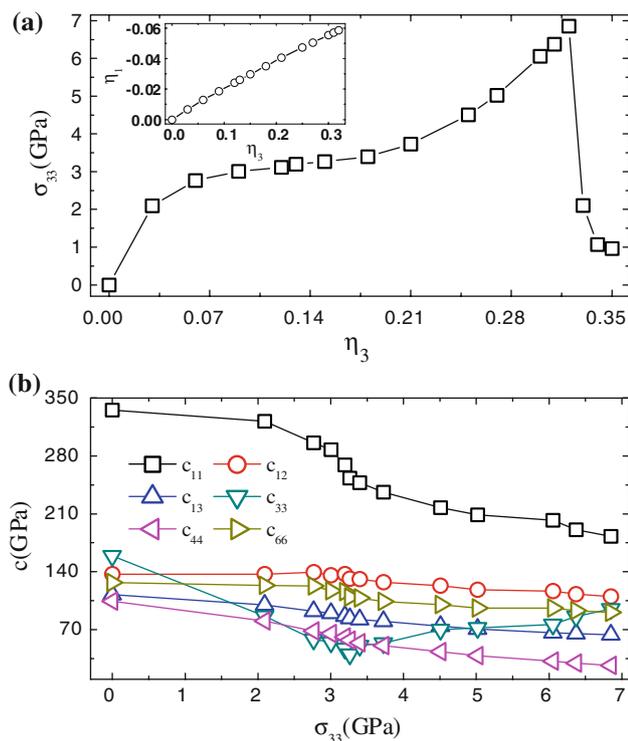
(a)

(b)

Fig. 2 **a** Uniaxial tensile stress as a function of tensile strain η_3, and the inset reflects the relation between strains η_3 and η_1. **b** Elastic constants as a function of stress σ_{33}

$\sigma_c = 3.26$ GPa and then gradually increases, promising a large electromechanical response at σ_c [27]. The minimum c_{33} corresponds to the minimum slope of the curve of Fig. 2a at σ_c. Other elastic constants, especially c_{11}, always decrease with increasing σ_{33}, indicating that the superlattice under the loading of uniaxial tensile stress along the c axis becomes soft along the nonpolar axes.

To illustrate the change of chemical bonds with uniaxial tensile stress, Fig. 3a and b are plotted to show the valence charge density along the c axis in the (100) and (200) planes of the superlattice at equilibrium, maximum piezoelectric coefficient and ideal tensile strength, respectively. The Pb $-$ O_4, Ba $-$ O_1, Ti_1-O_1 and Ti_2-O_4 bond lengths are not sensitive to the uniaxial tensile stress along the c axis, suggesting that the orbital hybridizations between these atoms are not sensitive to the uniaxial strain, whereas the Ti_1-O_3 and Ti_2-O_6 bonds elongate remarkably with increasing stress. Following the evolution of the charge density, we find that the weak Ti_1-O_3 bond starts to break first, followed by the Ti_2-O_6 bond. After the bond breaks, the system converts into a planar structure with alternating layers. On the other hand, Fig. 3a and b show that the valence charge density becomes more and more unsymmetrical with the uniaxial tensile stress increasing, indicating the increase in polarization. To confirm this, we have directly calculated the relations between the

polarization and the uniaxial tensile stress with the Berry-phase approach.

Figure 4a shows the polarization as a function of uniaxial tensile stress. For the ground state superlattice, the calculated spontaneous polarization of 0.29 C/m^2 is less than the theoretical value of 0.81 C/m^2 of ground state PTO, but slightly larger than the value of 0.28 C/m^2 of tetragonal BTO (the other theoretical value is 0.26 C/m^2 [28]), which supports the conclusion that the sharp interfaces suppress the polarization in short-period BTO/PTO superlattices [28]. As the stress σ_{33} increases, the polarization dramatically increases with the maximum slope appearing at σ_c, indicating that the ferroelectric phase becomes more and more stable with respect to the paraelectric phase. Figure 4b shows the variation of piezoelectric coefficients with stress σ_{33}, which are calculated by the linear response theory. The piezoelectric coefficients all increase with increasing σ_{33} and reach their maximum values at σ_c, indicating that the appropriately applied uniaxial tensile stress can enhance the piezoelectricity for the superlattice. The piezoelectric coefficient d_{33} of ground state superlattice is 86.36 pC/N, which is slightly less than the value of 103.18 pC/N of PTO, but much larger than the value of 36.43 pC/N of BTO. Under the loading of uniaxial tensile stress applied along the c axis, d_{33} is increased from its ground state value by a factor of about 8, reaching 678.42 pC/N for the superlattice. From previous calculations [14], we know that the uniaxial tensile stress can only enhance d_{33} of PTO to the maximum value of 380.50 pC/N. The enhancement of piezoelectricity is supported by the conclusion of uniaxial tensile stress dependency of elastic constant c_{33} (see Fig. 2b). Note that the polarization under uniaxial stress remains along the <001> direction and that the piezoelectric coefficients reflect the slope of polarization versus stress curves. The enhancement of piezoelectricity corresponds to the maximum slope of the curve of Fig. 4a at σ_c, it is the change of magnitude of polarization that leads to the enhancement of piezoelectricity.

To reveal the underlying mechanisms for the abnormal piezoelectricity, we study the effects of uniaxial tensile stress on the Born effective charges and atomic displacements, respectively (see Fig. 5a, b). Since the atomic displacements and polarization are all along the c axis, only charges Z^*_{zz} contribute to the polarization. The uniaxial tensile stress reduces the effective charges, which remain almost constant when $\sigma_{33} > \sigma_c$. The charges Z^*_{zz} of O_1 and O_4 atoms are much close to their normal charges, so does the case of Ti atoms when $\sigma_{33} > \sigma_c$, whereas Z^*_{zz} of O_3 and O_6 atoms are anomalously large compared with their normal charges, suggesting the strong orbital hybridization between Ti_1 (and Ti_2) $3d$ and O_6 (and O_3) $2p$ states (see Fig. 3b). Note that the Ba atom is fixed at (0, 0, 0) during the first-principles simulations. The displacements of O

Fig. 3 Calculated valence charge density along the *c* axis in the (100) (**a**) and (200) (**b**) planes of superlattice at equilibrium (*1*), maximum piezoelectric coefficient (*2*) and ideal tensile strength (*3*)
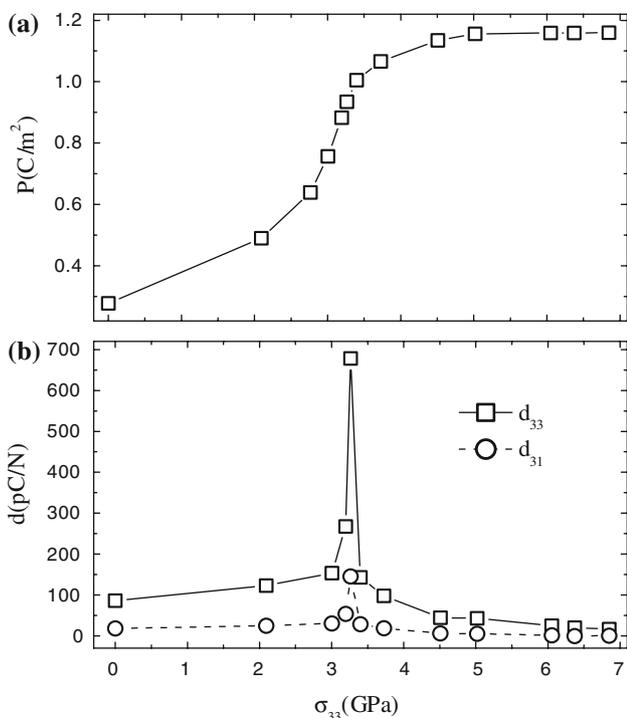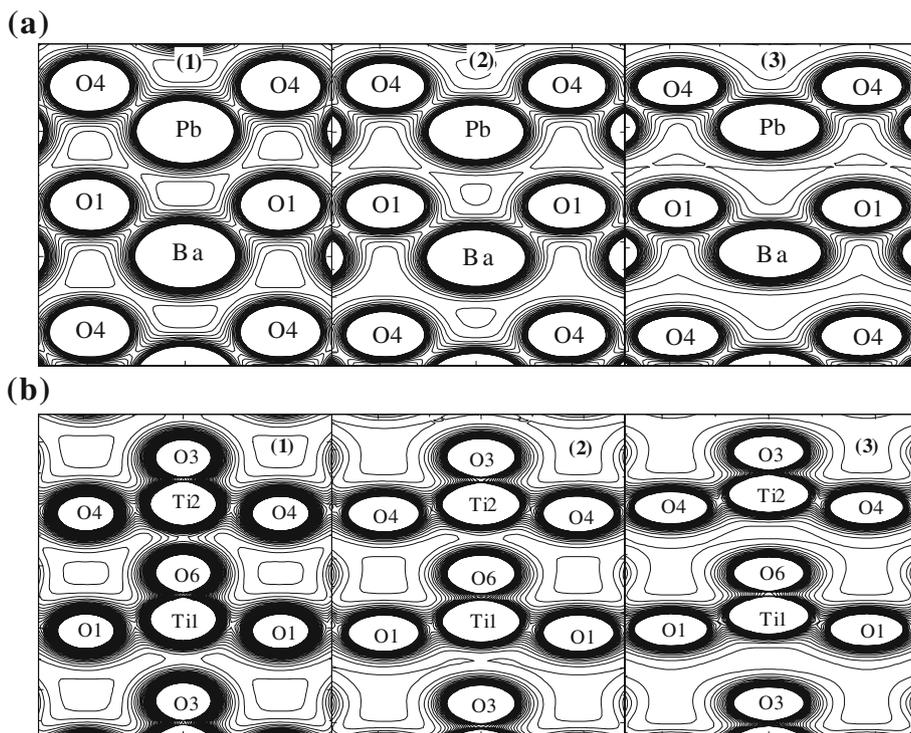

Fig. 4 Uniaxial tensile stress dependence of **a** polarization and **b** piezoelectric coefficients (i.e., d_{31} and d_{33})
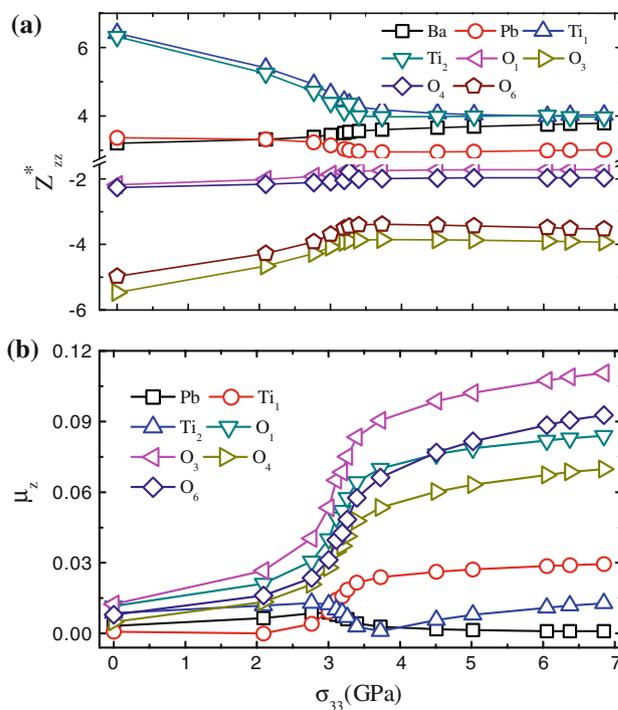
Fig. 5 a Born effective charges Z_{zz}^* and **b** atomic displacements along the *c* axis (in *c* units), relative to the centrosymmetric reference structure, as a function of uniaxial tensile stress

atoms, which are much larger than those of Pb and Ti atoms for a broad range of stress, are greatly enhanced as the stress σ_{33} increases, especially near σ_c, leading to the drastic increase in polarization. It is concluded that as the

stress σ_{33} increases, the atomic displacements are so greatly enhanced that the overall effect is the increase in polarization, even though the magnitudes of Z_{zz}^* decrease with the stress increasing.

Summary

In summary, we have studied the influence of uniaxial tensile stress applied along the c axis on the mechanical and piezoelectric properties of short-period BTO/PTO superlattice using first-principles methods. We show that the calculated ideal tensile strength is 6.850 GPa and that the superlattice under the loading of uniaxial tensile stress becomes soft along the nonpolar axes. We also find that the appropriately applied uniaxial tensile stress can significantly enhance the piezoelectricity for the superlattice. Our calculated results reveal that it is the drastic increase in atomic displacements along the c axis that leads to the increase in polarization and that the enhancement of piezoelectricity is attributed to the change in the magnitude of polarization with the stress. Our work suggests a way of enhancing the piezoelectric properties of the superlattices, which would be helpful to enhance the performance of the piezoelectric devices.

References

1. M.E. Lines, A.M. Glass, Principles and Applications of Ferroelectrics and Telated Materials. (Clarendon, Oxford, 1979)
2. K. Uchino, Piezoelectric Actuators and Ultrasonic Motors. (Kluwer, Boston, 1996)
3. Z. Zhu, H. Zhang, M. Tan, X. Zhang, J. Han, J. Phys. D: Appl. Phys. **41**, 215408 (2009)
4. W. Zhong, D. Vanderbilt, K.M. Rabe, Phys. Rev. B **52**, 6301 (1995)
5. H. Salehi, N. Shahtahmasebi, S.M. Hosseini, Eur. Phys. J. B **32**, 177 (2003)
6. G.A. Samara, T. Sakudo, K. Yoshimitsu, Phys. Rev. Lett. **35**, 1767 (1975)
7. R.E. Cohen, Nature **358**, 136 (1992)
8. H. Fu, R.E. Cohen, Nature **403**, 281 (2000)
9. Z. Wu, R.E. Cohen, Phys. Rev. Lett. **95**, 037601 (2005)
10. Y. Sang, B. Liu, D. Fang, Chin. Phys. Lett. **25**, 1113 (2008)
11. C. Ederer, N.A. Spaldin, Phys. Rev. Lett. **95**, 257601 (2005)
12. Y. Duan, J. Li, S.-S. Li, J.-B. Xia, C. Chen, J. Appl. Phys. **103**, 083713 (2008)
13. C. Wang, Y. Duan, C. Chen, Chin. Phys. Lett. **26**, 017203 (2009)
14. Y. Duan, H. Shi, L. Qin, J. Phys.: Condens. Matter **20**, 175210 (2008)
15. Y. Duan, L. Qin, G. Tang, C. Chen, J. Appl. Phys. **105**, 033706 (2009)
16. Z. Li, T. Lu, W. Cao, J. Appl. Phys. **104**, 126106 (2008)
17. B. Neaton, K.M. Rabe, Appl. Phys. Lett **82**, 1586 (2003)
18. S.H. Shah, P.D. Bristowe, A.M. Kolpak, A.M. Rappe, J. Mater. Sci. **43**, 3750 (2008)
19. X. Gonze, J.-M. Beuken, R. Caracas, F. Detraux, M. Fuchs, G.-M. Rignanese, L. Sindic, M. Verstraete, G. Zerah, F. Jollet, M. Torrent, A. Roy, M. Mikami, Ph. Ghosez, J.-Y. Raty, D.C. Allan, Comput. Mater. Sci. **25**, 478 (2002)
20. A.M. Rappe, K.M. Rabe, E. Kaxiras, J.D. Joannopoulos, Phys. Rev. B **41**, 1227 (1990)
21. D.J. Singh, Planewaves, Pseudopotential, and the LAPW Method. (Kluwer, Boston, MA, 1994)
22. X. Gonze, C. Lee, Phys. Rev. B **55**, 10355 (1997)
23. S. Baroni, S. de Gironcoli, A. Dal Corso, P. Giannozzi, Rev. Mod. Phys. **73**, 515 (2001)
24. D.R. Hamann, X. Wu, K.M. Rabe, D. Vanderbilt, Phys. Rev. B **71**, 035117 (2005)
25. R.D. King-Smith, D. Vanderbilt, Phys. Rev. B **47**, 1651 (1993)
26. Z. Wu, R.E. Cohen, D.J. Singh, Phys. Rev. B **70**, 104112 (2004)
27. Z. Alahmed, H. Fu, Phys. Rev. B **77**, 045213 (2008)
28. V.R. Cooper, K.M. Rabe, Phys. Rev. B **79**, 180101 (2009)